

Metrics for Molecular Electronic Excitations: A Comparison between Orbital- and Density-Based Descriptors

Marika Savarese,[†]Ciro Achille Guido,[‡] Eric Brémond,[†]Ilaria Ciofini,[§] and Carlo Adamo^{*,§}

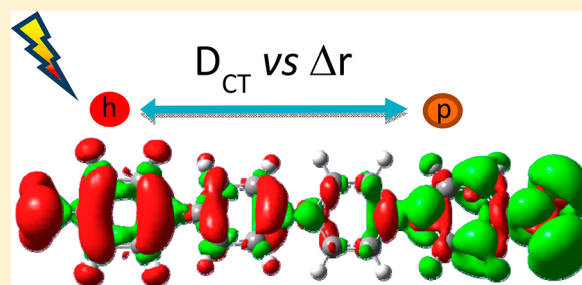
[†]CompuNet, Istituto Italiano di Tecnologia, via Morego 30, I-16163 Genoa, Italy

[‡]Laboratoire CEISAM—UMR CNRS 6230, Université de Nantes, 2 Rue de la Houssinière, 44322 Nantes Cedex 3, France

[§]Chimie ParisTech, PSL Research University, CNRS, Institut de Recherche de Chimie Paris, F-75005 Paris, France

S Supporting Information

ABSTRACT: This study proposes a quantitative and qualitative comparison of two popular metrics used for time-dependent density functional simulations of chromophores when describing absorption and emission processes, with high discrimination power between short- and long-range character of involved electronic excitations and functional performances. To this end, a total of 160 absorption and emission electronic excitations of 80 molecular systems belonging to the “Real-Life Molecules” data set, recently introduced in literature, have been considered a relevant data set. The two selected indexes are based on density (the D_{CT} one) and natural transition orbitals (the Δr_{NTO} one), respectively. For comparison purposes, an extension of the D_{CT} index, in line with what exists for Δr_{NTO} , enabling to discriminate electronic transitions occurring in symmetric systems is also proposed. The results show that, independently of the exchange and correlation functional used, a good correlation between the natural transition orbital and density based descriptors is found, thus cross validating their use for the quantification of a large variety of transitions in chemically relevant molecular systems.



1. INTRODUCTION

Time-dependent density functional theory (TD-DFT)¹ is nowadays largely used to study light-induced phenomena, especially in molecular systems, due to its very favorable accuracy to cost ratio. As a consequence, the DFT community is intensively working on benchmarking its numerical performances in predicting the absorption energy (see, for instance, refs 2–4) or in computing emission energies (see for instance refs 5–7) on large data sets of representative molecules. During the years, this huge effort allowed to clearly highlight some drawbacks of this method. Among others, the problem related to the incorrect estimation of electronic excitations with relevant charge transfer (CT) character is of particular relevance for chemical applications, and it is well documented in the literature.^{8,9} Its origin resides in the approximate nature of the exchange-correlation functionals,^{10,11} and it can not only affect the computed CT energies but it could also lead to the prediction of low lying unphysical excited states, defined as “ghost states”.^{8,12} Therefore, beyond assessing the numerical accuracy of different DFT functionals, a significant effort was focused on the development of diagnostic indexes, enabling to spot the erroneous behavior of TD-DFT calculations.

In this field, the seminal work of Gritsenko and Baerends¹⁰ was followed by the development of the Λ index by Tozer and collaborators.^{13,14} The Λ index roughly measures the degree of spatial overlap between occupied and virtual orbitals involved in a given electronic transition, so that a small (null) overlap corresponds to problematic transitions, as CT excitations.¹⁴

Following these works, more recently, several indexes were also developed with the aim of describing, and possibly quantifying, the nature of a given electronic excitation, though not necessarily providing diagnostic tools for TD-DFT. These tools can be grouped in two distinct families, one based on electron density and another one based on molecular orbitals. To the first family can be ascribed approaches based on detachment/attachment densities,¹⁵ on the density overlap region indicator scalar field,¹⁶ or density partitions (e.g., atomic charges).^{17–19} The second group²⁰ can be classified as the already mentioned Λ index and another one based on charge centroids.^{21,22} All these methods present their own pro and cons,²³ but it could be expected a certain degree of correlation in their outcomes, due to the strong connection between the underpinning variables, that is electron densities and molecular orbitals. Following this line, already evidenced in chemical bonding analysis some years ago,²⁴ we will focus on the comparison of two metrics, one based on molecular orbital and another one on electron density, in order to assess to which extent the picture provided by these two approaches is qualitatively and quantitatively comparable.

As an orbital-based metric, that proposed by Guido and Adamo (the so-called Δr , refs 21 and 22) is here considered since it enables to describe and quantify the displacement of

Received: July 18, 2017

Revised: September 9, 2017

Published: September 12, 2017

orbital centroids providing an intuitive picture of the effective electron displacement during the electronic transitions, particularly in its natural transition orbital version (Δr_{NTO}). The Δr index has been used to evaluate the CT character of organic chromophores^{25–28} and to rationalize the singlet–triplet gap in organic light-emitting diode (OLED) materials,²⁹ and a relationship between this metrics and nonlinear optical properties of push–pull systems was recently provided.³⁰ Moreover, its definition has been also extended to tight binding TD-DFT,³¹ and it has also been implemented in an open-source code.³²

As density-based description, the first density-based quantification of CT length, proposed by Le Bahers and Ciofini in 2011 (the so-called D_{CT} , ref 19) will be then considered. In this case, the spatial extent associated with a given electronic excitation is computed from the position of the barycenters of charges computed for the electron and the hole produced by the excitation. This latter index has been used to evaluate the CT character of electronic transition especially in the field of push–pull chromophores^{33–35} and, more generally, in organic dyes for assorted applications.^{36–41} Furthermore, other descriptors derived from the original D_{CT} have been formulated for the description of photophysical behavior and reactivity of molecular systems.^{42,43} Due to its simple formulation and its intuitive use, it has also been implemented in different computational packages.^{32,44}

In this article, we compare the behavior of these two metrics in estimating the excitation character of the absorption and emission of the molecules belonging to the large “80 Real-Life Compounds” data set (hereafter labeled RLex80), which encompasses several types of molecules and excitations, including some difficult cases such as charge-transfer systems, push–pull structures, and cyanine-like dyes.⁴⁵ The effect of the density functional on the obtained results was also checked by considering four different exchange–correlation functionals, belonging to different types of approximations and chosen among those commonly used.

2. THEORY AND COMPUTATIONAL DETAILS

Molecules included in the RLex80 data set⁴⁵ are sketched in Figure S1. Both absorption and emission transitions are here considered for a total of 160 transitions. Ground and excited state minimum energy structures were obtained at the DFT and TD-DFT level using the M06-2X functional and the 6-31+G(d) basis set.⁴⁶

To compute electronic excitations and indexes, we have selected four different exchange correlation functionals: (i) the PBE functional,⁴⁷ belonging to the Generalized Gradient Approximation (GGA), and (ii) the corresponding parameter-free Global Hybrid (GH) PBE0 including 25% of exact EXchange (EXX),⁴⁸ (iii) a commonly used GH with higher EXX contribution (M06-2X, EXX = 54%),⁴⁶ and (iv) the ω B97XD⁴⁹ Range Separated Hybrid (RSH) proposed in the literature as a good compromise to predict position and vibronic shape of absorption bands.⁵⁰

All the calculations were carried out with the 6-31+G(d) basis set, a basis that provides converged excitations.⁵¹

For an extensive description of the formulation of orbital and density-based indexes, we refer the reader to the original papers.^{19,21,22} Here, for the sake of clarity, we will only recall their general expressions.

Having defined $\rho_{\text{GS}}(r)$ and $\rho_{\text{EX}}(r)$ as the ground and excited state electronic density, respectively, and the density rearrange-

ment associated with an electronic excitation ($\Delta\rho(r)$) as their difference (that is $\Delta\rho(r) = \rho_{\text{EX}}(r) - \rho_{\text{GS}}(r)$), two functions ($\rho_+(r)$ and $\rho_-(r)$) can be defined as the regions where an increase (or depletion) of the electronic density upon excitation is produced. Therefore

$$\rho_+(r) = \begin{cases} \Delta\rho(r) & \text{if } \Delta\rho(r) > 0 \\ 0 & \text{if } \Delta\rho(r) < 0 \end{cases} \quad \rho_-(r) = \begin{cases} \Delta\rho(r) & \text{if } \Delta\rho(r) < 0 \\ 0 & \text{if } \Delta\rho(r) > 0 \end{cases} \quad (1)$$

The spatial distance between the barycenters (referred in the following as \mathbf{R}_+ and \mathbf{R}_-) of these $\rho_+(r)$ and $\rho_-(r)$ distributions defines the D_{CT} index as

$$D_{\text{CT}} = |\mathbf{R}_+ - \mathbf{R}_-| \quad (2)$$

A measure of the spreading of the $\rho_+(r)$ and $\rho_-(r)$ regions can be given computing the root-mean-square deviations along the three axes (σ_{aj} where $a = +$ or $-$, $j = x, y, z$, and i indicates the grid points) as

$$\sigma_{aj} = \sqrt{\frac{\sum_i \rho_a(r_i)(j - j_a)^2}{\sum_i \rho_a(r_i)}} \quad (3)$$

Finally, the difference in spreading between electron and hole distributions can be defined as

$$\Delta\sigma_{\text{CT}} = |\sigma_+ - \sigma_-| \quad (4)$$

This index, contrary to D_{CT} , does not necessarily vanish for symmetric systems, but it has no physical relation with a charge transfer distance, as D_{CT} has.

Using the orbital based formalism, the charge transfer distance is defined by the means of the Δr index as follows:²¹

$$\Delta r = \frac{\sum_{ia} K_{ia}^2 |\langle \varphi_a | r | \varphi_i \rangle - \langle \varphi_i | r | \varphi_a \rangle|}{\sum_{ia} K_{ia}^2} \quad (5)$$

where i and a are, respectively, the occupied and virtual orbitals, $|\langle \varphi_p | r | \varphi_q \rangle|$ represent the norm of the orbital centroid, and K_{ia} is the sum of excitation and de-excitation coefficients of the random phase approximation of TD-DFT equations:

$$K_{ia}^2 = X_{ia}^2 - Y_{ia}^2$$

In this case, the spreading around the centroid of charges can be defined as the root-mean-square deviation of the position operator:²²

$$\sigma_p = \sqrt{\langle \varphi_p | r^2 | \varphi_p \rangle - \langle \varphi_p | r | \varphi_p \rangle^2} \quad (6)$$

The $\Delta\sigma$ can then be defined as

$$\Delta\sigma = \frac{\sum_{ia} K_{ia}^2 |\sigma_a - \sigma_i|}{\sum_{ia} K_{ia}^2} \quad (7)$$

Molecular-orbital based indexes were obtained using either the canonical molecular orbitals or the Natural Transition Orbitals (NTO),⁵² as provided by a locally modified version of the Gaussian⁵³ development code. When not differently specified, density-based indexes have been computed using relaxed densities and using a freely available in-house developed software.⁵⁴

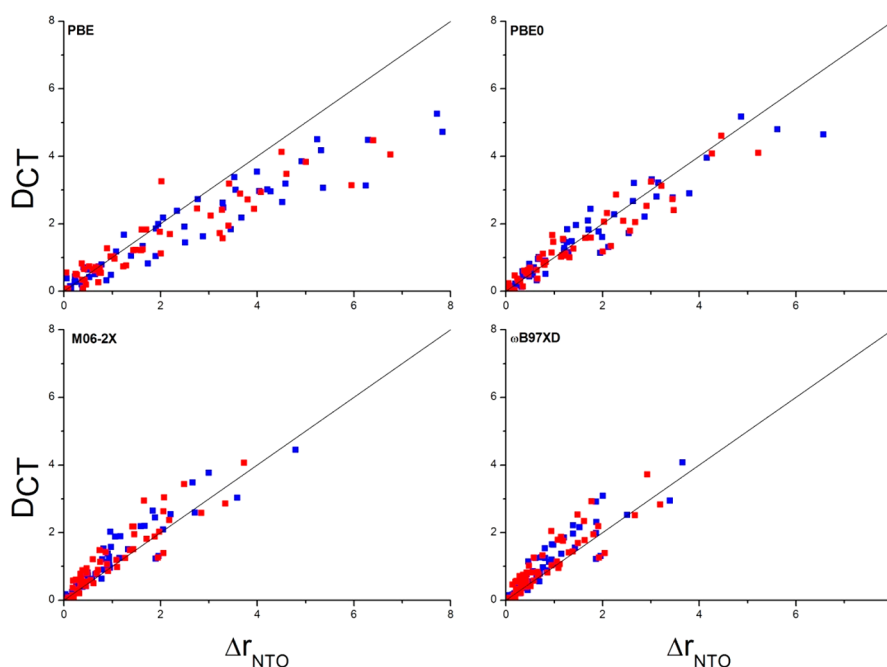


Figure 1. Correlation between D_{CT} and Δr_{NTO} indexes (in Å) computed at the PBE, PBE0, M06-2X, and ω B97XD level for absorption (in blue square) and emission (in red square). Only noncentrosymmetric molecules are reported. Straight line corresponds to slope = 1.

3. RESULTS

As first step, we analyze how the computed D_{CT} (eq 2) and Δr (eq 5) correlate when absorption and emission energies are evaluated at different levels of theory, namely, using the four selected functionals, since as already pointed out in precedent studies they could have a nonnegligible effect on the CT character of the computed transitions.^{13,17,55} The results obtained are reported in Figure 1. Please note that, in order to have a more relevant statistical analysis, all centrosymmetric molecules have been removed from the data set together with all those molecules possessing a D_{CT} smaller than 0.05 Å. This reduced data set corresponds to a total of more than 50 molecules for each functional (i.e., 55 molecules for PBE, 53 for PBE0, 52 for M06-2X, and 60 for ω B97XD). From inspection of Figure 1, an overall good correlation between D_{CT} and Δr can be found, the R^2 ranging from 0.93 (ω B97XD) to 0.86 (M06-2X) for absorption and from 0.91 (ω B97XD) to 0.84 (M06-2X). More interestingly, the slope of the linear regression is slightly larger than 1 for M06-2X and ω B97XD for both absorption and emission, while it is less than 0.9 for PBE0 and about 0.7 for PBE. This behavior is apparent from the plots of Figure 1, where the variations with respect to a perfect correlation (slope = 1) are evident for PBE and, to a minor extent, for PBE0. It is dominated by “long range” CT excitations, i.e., those with high D_{CT} and Δr values, where the correlation between D_{CT} and Δr appears to degrade. In more detail, at the PBE level, while for local transitions (i.e., low CT distances) the two indexes correlate quite well, for transitions with high CT character, the D_{CT} analysis provides charge transfer distances that are systematically smaller than those computed by Δr . The increase of the EXX contribution, either in GHs or RSH, improves the agreement between the two sets and provides transition energies in better agreement with the reference CC2 calculations (see Table S1). A similar trend was already noticed for the D_{CT} based metric.³⁴ As expected, the inclusion of centrosymmetric systems improves

the linear relationship between Δr and D_{CT} . Indeed, R^2 ranges from 0.94 (PBE) to 0.89 (ω B97XD) for absorption and from 0.93 (PBE0) to 0.86 (ω B97XD) for emission.

In order to gain some insights on the origin of this systematic underestimation of CT length provided by D_{CT} with respect to the Δr metrics, we focused on four molecules: two (labeled 17 and 26, Figure 2) as representative of chromophores possessing

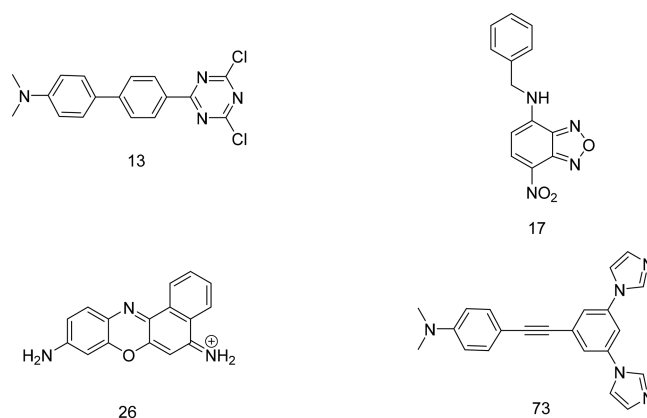


Figure 2. Sketches of the four selected molecules extracted from the large RLex80 data set for a deeper analysis (see text for details).

locally excited (LE) states and two systems (13 and 73 in Figure 2) displaying long-range CT transitions. Since the same qualitative trend is observed for both absorption and emission, for detailed analysis we will focus only on the indexes computed for absorption transitions as reported in Figure 3 (panel A). The two general features already observed for the full data set can be here more clearly spotted. Indeed, for transition with LE character (molecules 17 and 26), all functionals predict almost equivalent charge transfer distances, and an almost linear correlation between D_{CT} and Δr is found. However, for systems characterized by transitions with a

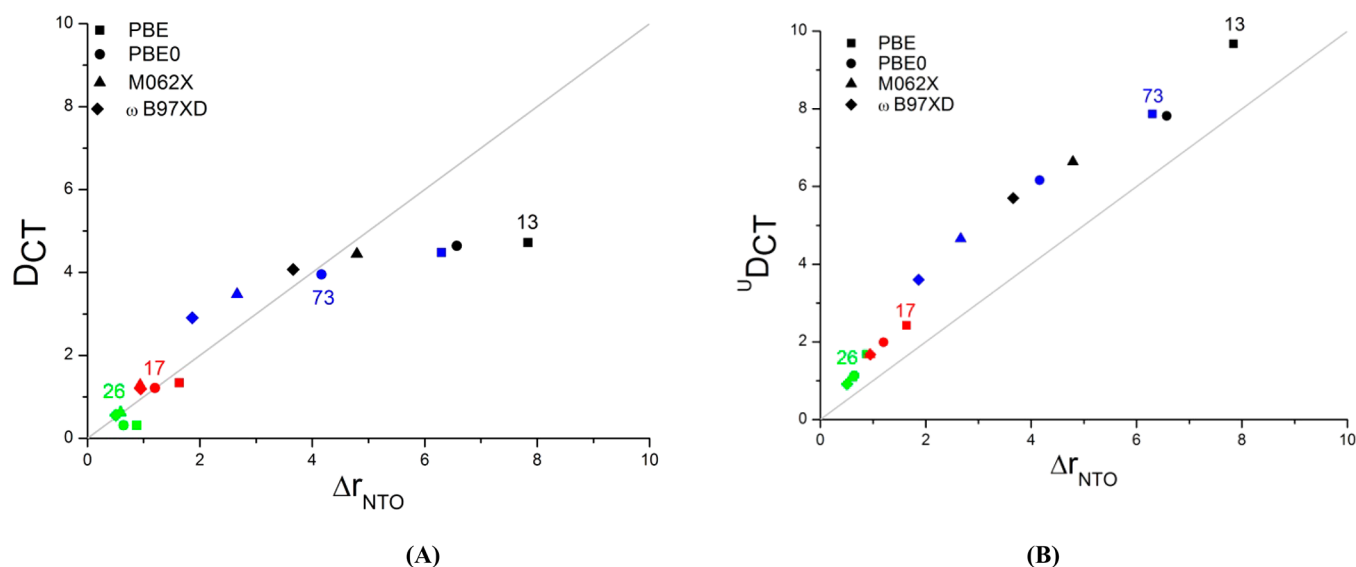


Figure 3. Correlation between D_{CT} and $\Delta \rho_{NTO}$ indexes (A, in Å) and $^U D_{CT}$ and $\Delta \rho_{NTO}$ indexes (B, in Å) computed with the PBE, PBE0, M06-2X, and ω B97XD density functionals for selected molecule absorption (13 in black, 17 in red, 26 in green, and 73 in blue).

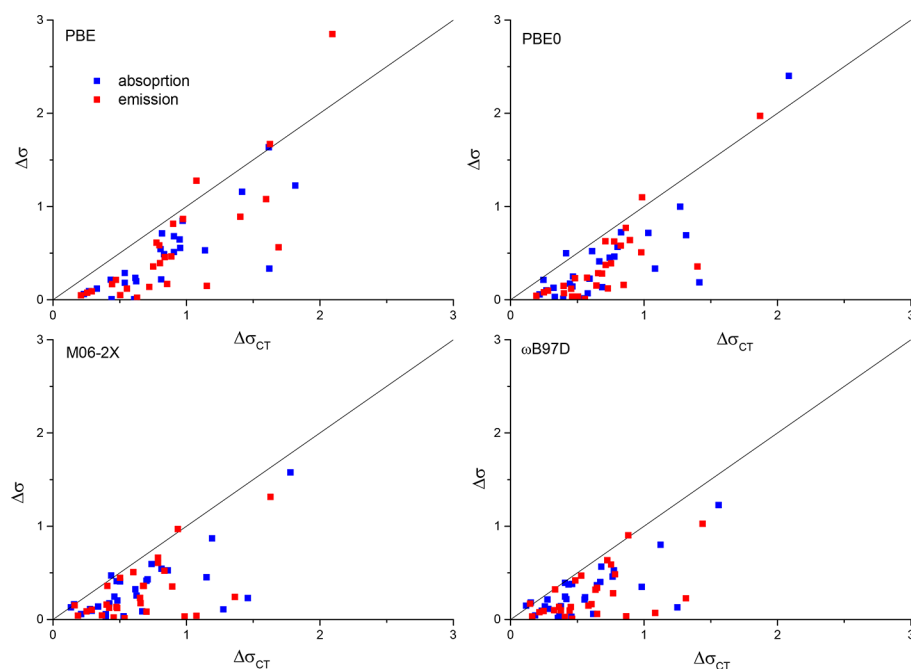


Figure 4. Correlation between $\Delta \sigma_{CT}$ and $\Delta \sigma$ for all the centrosymmetric molecules. Data have been computed for absorption (blue square) and emission (red square) using the four selected functionals (PBE, PBE0, M06-2X, and ω B97XD).

relevant CT character (13 and 73), a spreading of both Δr and D_{CT} values is observed, depending on the functional used. Nonetheless, Δr is clearly more sensitive than D_{CT} to the functional used, as electron density is only marginally affected by the chosen DFT approach.⁵⁶ The higher CT character is related to the different description provided by the functionals used: GGAs or functionals with a low EXX contribution predict CT at longer distances.

Clearly for high CT length, Δr is systematically larger than D_{CT} . A possible explanation relies on the way the two indexes are computed: the D_{CT} discussed up to now makes use of relaxed excited state densities, while Δr is computed from NTOs, which are a single value decomposition of the single particle transition density matrix associated with the excited

state. Indeed, for the purposes of a more straightforward comparison, it is possible to compute the D_{CT} index considering the unrelaxed part of the one-particle excited state density ρ_{ES} . The corresponding index will be labeled $^U D_{CT}$. The correlation between $^U D_{CT}$ and Δr is also reported in Figure 3 (panel B). The data show that $^U D_{CT}$ better correlates with Δr_{NTO} independently on the functional used and on the range of CT length considered, even if based on two different quantities: i.e. unrelaxed excited state and transition density matrixes. Nonetheless, it should be stressed that the description of the excited state provided by the use of relaxed densities (and therefore of the standard D_{CT}) is in principle more accurate than that provided by unrelaxed densities.^{57,58} Therefore, for transition of high CT character, the use of

relaxed D_{CT} should be preferred with respect to the use of $^U D_{CT}$ or Δr_{NTO} , while for transitions with less relevant CT character, D_{CT} and Δr_{NTO} can both be safely used.

As previously mentioned, by construction both D_{CT} and Δr_{NTO} metrics vanish in the case of centrosymmetric molecules. In order to compare the two metrics for such systems, we have considered the two indexes related to the spreading of the positive and negative density regions ($\Delta\sigma_{CT}$, eq 4) and of the charge centroids ($\Delta\sigma$, eq 7). The correlation plots computed for the absorption and emission transitions of 27 (see Table S2 for a list) centrosymmetric molecules are reported in Figure 4. As it can be seen from these data, the $\Delta\sigma_{CT}$ values are generally higher than the corresponding $\Delta\sigma$, thus suggesting a larger anisotropy of the density upon excitations, not always caught by the molecular orbitals. This trend is observed for absorption and emission, and it is valid for all the considered functionals. Nonetheless, a general contraction of the values is observed in going from PBE to ω B97XD. As before, the increase of the EXX contribution into the functional plays a significant role on the computed indexes. Looking more in detail, it can be observed that some molecules are particularly affected. For instance, the $\Delta\sigma_{CT}$ computed at the PBE level for the absorption transition of 58 (see Figure S1) is 1.62 Å, while $\Delta\sigma$ is about five times smaller (0.33 Å). A similar behavior is found with other functionals, even if the discrepancy decreases with the increasing of the EXX contribution. Indeed, the difference between the two indexes is slightly lower at the M06-2X level (1.27 vs 0.11 Å). Interestingly, emission shows smaller values (1.15 and 0.15 for $\Delta\sigma_{CT}$ and $\Delta\sigma$, respectively, at the PBE level).

One molecule, 78, is characterized by high values of both indexes at the PBE level: 2.3 and 3.2 Å for $\Delta\sigma_{CT}$ and $\Delta\sigma$, respectively, for absorption and 2.1 and 2.9 Å for emission. Nevertheless, the inclusion of EXX significantly decreases these values. For instance, at the M06-2X level, $\Delta\sigma_{CT}$ and $\Delta\sigma$ for the absorption are 1.78 and 1.59 Å, respectively.

All these trends could be ascribed to the use of relaxed densities for $\Delta\sigma_{CT}$ and unrelaxed orbitals for $\Delta\sigma$, as already discussed for D_{CT} . Indeed, Δr and the associated $\Delta\sigma$ are not invariant with respect to the molecular orbital basis. In the original formulation,²¹ $\Delta\sigma$ was evaluated using the canonical MOs, while in the subsequent evolution, the more robust NTO approach was considered.²² Indeed, NTOs give a more compact orbital representation, so that a maximal correspondence exists between the excited “particle” and the empty “hole”. The qualitative agreement between D_{CT} , which is the average distance between the particle and the hole, and Δr , computed using NTO, confirms this point of view. Nevertheless, it is interesting to compare, for noncentrosymmetric molecules, the two basis, canonical MOs and NTOs, for computing Δr . The results obtained with the ω B97XD functional, reported in Figure 5, well evidence the effect of using the more-compact NTOs, the corresponding Δr values being smaller than those obtained with the original formulation. For instance, the electronic transition computed for molecule 12 is characterized by a high value of $\Delta r(MO)$ (6.2 Å, the point on the extreme right in Figure 5), while $\Delta r(NTO)$ is significantly smaller (3.7 Å). It is then reassuring that, for the same molecule, the D_{CT} is 4.1 Å, further validating the robustness of the orbital-based descriptor $\Delta r(NTO)$ and its good quantitative agreement with the density-based index, D_{CT} .

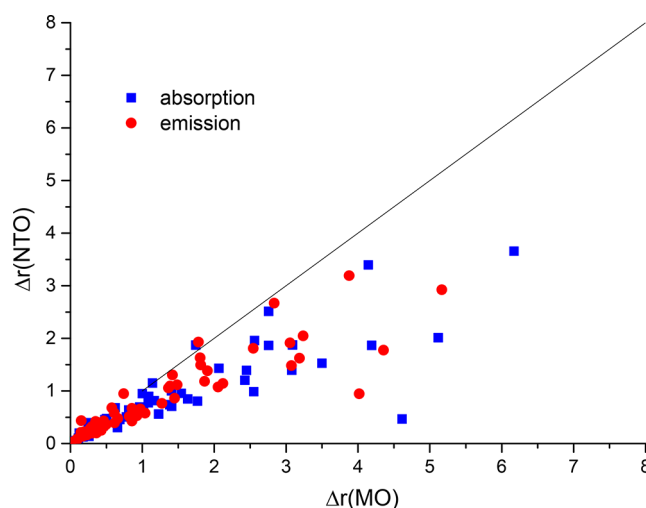


Figure 5. Correlations between $\Delta\sigma$ computed on the basis of Natural Transition Orbitals ($\Delta\sigma(NTO)$) and $\Delta\sigma$ computed using canonical Molecular Orbitals ($\Delta\sigma(MO)$) for absorption (blue square) and emission (red square).

4. CONCLUSIONS

The use of a valuable computational tool like TD-DFT for the evaluation of absorption and emission energies requires the simultaneous consideration of diagnostic indexes in order to detect problematic cases and to allow for straightforward routine use, even by nonspecialized researchers. Among others, two indexes, one based on molecular orbitals, Δr , and another one based on electron density, D_{CT} , have been proven to be particularly robust for detecting CT excitations, one of weak points of TD-DFT approximations. In this article, we have proposed a detailed comparison between these two indexes considering a large set of test molecules and both absorption and emission transitions. Furthermore, these indexes have been computed using four different functionals, among the most used ones. The obtained results suggest that, when the Δr index is computed on the basis of the Natural Transition Orbitals, a good correlation is obtained with D_{CT} , even if the former indicates larger CT than the latter. Furthermore, D_{CT} is less affected by the functional choice than Δr . Centrosymmetric molecules have been also tackled using two descriptors to evaluate the spreading between electron and hole distributions.

■ ASSOCIATED CONTENT

Supporting Information

The Supporting Information is available free of charge on the ACS Publications website at DOI: 10.1021/acs.jpca.7b07080.

Sketches of the test molecules, statistics on the computed vertical absorption and emission transitions, list of the centrosymmetric molecules, and complete references 44 and 53 (PDF)

■ AUTHOR INFORMATION

Corresponding Author

*E-mail: carlo.adamo@chimie-paristech.fr.

ORCID

Marika Savarese: 0000-0002-4609-9603

Eric Brémond: 0000-0002-8646-9365

Ilaria Ciofini: 0000-0002-5391-4522

Carlo Adamo: 0000-0002-2638-2735

Notes

The authors declare no competing financial interest.

ACKNOWLEDGMENTS

This project has received funding from the European Research Council (ERC) under the European Union's Horizon 2020 research and innovation program (grant agreement No. 648558).

REFERENCES

- (1) Runge, E.; Gross, E. K. U. Density-Functional Theory for Time-Dependent Systems. *Phys. Rev. Lett.* **1984**, *52*, 997–1000.
- (2) Schreiber, M.; Silva-Junior, M. R.; Sauer, S. P. a; Thiel, W. Benchmarks for Electronically Excited States: CASPT2, CC2, CCSD, and CC3. *J. Chem. Phys.* **2008**, *128*, 134110.
- (3) Jacquemin, D.; Wathelet, V.; Perpète, E. A.; Adamo, C. Extensive TD-DFT Benchmark: Singlet-Excited States of Organic Molecules. *J. Chem. Theory Comput.* **2009**, *5*, 2420–2435.
- (4) Leang, S. S.; Zahariev, F.; Gordon, M. S. Benchmarking the performance of time-dependent density functional methods. *J. Chem. Phys.* **2012**, *136*, 104101.
- (5) Guido, C. A.; Knecht, S.; Kongsted, J.; Mennucci, B. Benchmarking Time-Dependent Density Functional Theory for Excited State Geometries of Organic Molecules in Gas-Phase and in Solution. *J. Chem. Theory Comput.* **2013**, *9*, 2209–2220.
- (6) Bousquet, D.; Fukuda, R.; Maitard, P.; Jacquemin, D.; Ciofini, I.; Adamo, C.; Ehara, M. Excited-State Geometries of Heteroaromatic Compounds: A Comparative TD-DFT and SAC-CI Study. *J. Chem. Theory Comput.* **2013**, *9*, 2368–2379.
- (7) Bernini, C.; Zani, L.; Calamante, M.; Reginato, G.; Mordini, A.; Taddei, M.; Basosi, R.; Sinicropi, A. Excited State Geometries and Vertical Emission Energies of Solvated Dyes for DSSC: A PCM/TD-DFT Benchmark Study. *J. Chem. Theory Comput.* **2014**, *10*, 3925–3933.
- (8) Dreuw, A.; Head-Gordon, M. Failure of Time-Dependent Density Functional Theory for Long-Range Charge-Transfer Excited States: The Zincbacteriochlorin-Bacteriochlorin and Bacteriochlorophyll-Spheroidene Complexes. *J. Am. Chem. Soc.* **2004**, *126*, 4007–4016.
- (9) Dreuw, A.; Head-Gordon, M. Single-Reference Ab Initio Methods for the Calculation of Excited States of Large Molecules. *Chem. Rev.* **2005**, *105*, 4009–4037.
- (10) Gritsenko, O.; Baerends, E. J. Asymptotic Correction of the Exchange–Correlation Kernel of Time-Dependent Density Functional Theory for Long-Range Charge-Transfer Excitations. *J. Chem. Phys.* **2004**, *121*, 655–660.
- (11) Casida, M. E.; Jamorski, C.; Casida, K. C.; Salahub, D. R. Molecular Excitation Energies to High-Lying Bound States from Time-Dependent Density-Functional Response Theory: Characterization and Correction of the Time-Dependent Local Density Approximation Ionization Threshold. *J. Chem. Phys.* **1998**, *108*, 4439–4449.
- (12) Tawada, Y.; Tsuneda, T.; Yanagisawa, S.; Yanai, T.; Hirao, K. A Long-Range-Corrected Time-Dependent Density Functional Theory. *J. Chem. Phys.* **2004**, *120*, 8425–8433.
- (13) Peach, M. J. G.; Benfield, P.; Helgaker, T.; Tozer, D. J. Excitation Energies in Density Functional Theory: An Evaluation and a Diagnostic Test. *J. Chem. Phys.* **2008**, *128*, 044118.
- (14) Peach, M. J. G.; Tozer, D. J. Illustration of a TD-DFT Spatial Overlap Diagnostic by Basis Function Exponent Scaling. *J. Mol. Struct.: THEOCHEM* **2009**, *914*, 110–114.
- (15) Etienne, T.; Assfeld, X.; Monari, A. Toward a Quantitative Assessment of Electronic Transitions' Charge-Transfer Character. *J. Chem. Theory Comput.* **2014**, *10*, 3896–3905.
- (16) Vannay, L.; Brémond, E.; de Silva, P.; Corminboeuf, C. Visualizing and Quantifying Interactions in the Excited State. *Chem. - Eur. J.* **2016**, *22*, 18442–18449.
- (17) Ronca, E.; Pastore, M.; Belpassi, L.; De Angelis, F.; Angeli, C.; Cimraglia, R.; Tarantelli, F. Charge-Displacement Analysis for Excited States. *J. Chem. Phys.* **2014**, *140*, 054110.
- (18) Syzgantseva, O. A.; Tognetti, V.; Boulangé, A.; Peixoto, P. A.; Leleu, S.; Franck, X.; Joubert, L. Evaluating Charge Transfer in Epicoconone Analogues: Toward a Targeted Design of Fluorophores. *J. Phys. Chem. A* **2014**, *118*, 757–764.
- (19) Le Bahers, T.; Adamo, C.; Ciofini, I. A Qualitative Index of Spatial Extent in Charge-Transfer Excitations. *J. Chem. Theory Comput.* **2011**, *7*, 2498–2506.
- (20) Plasser, F.; Thomitzni, B.; Bäßler, S. A.; Wenzel, J.; Rehn, D. R.; Wormit, M.; Dreuw, A. Statistical Analysis of Electronic Excitation Processes: Spatial Location, Compactness, Charge Transfer, and Electron-Hole Correlation. *J. Comput. Chem.* **2015**, *36*, 1609–1620.
- (21) Guido, C. A.; Cortona, P.; Mennucci, B.; Adamo, C. On the Metric of Charge Transfer Molecular Excitations: A Simple Chemical Descriptor. *J. Chem. Theory Comput.* **2013**, *9*, 3118–3126.
- (22) Guido, C. A.; Cortona, P.; Adamo, C. Effective Electron Displacements: A Tool for Time-Dependent Density Functional Theory Computational Spectroscopy. *J. Chem. Phys.* **2014**, *140*, 104101.
- (23) Adamo, C.; Le Bahers, T.; Savarese, M.; Wilbraham, L.; García, G.; Fukuda, R.; Ehara, M.; Rega, N.; Ciofini, I. Exploring Excited States Using Time Dependent Density Functional Theory and Density-Based Indexes. *Coord. Chem. Rev.* **2015**, *304–305*, 166–178.
- (24) Petit, L.; Joubert, L.; Maldivi, P.; Adamo, C. A Comprehensive Theoretical View of the Bonding in Actinide Molecular Complexes. *J. Am. Chem. Soc.* **2006**, *128*, 2190–2191.
- (25) Guido, C. A.; Jacquemin, D.; Adamo, C.; Mennucci, B. Electronic Excitations in Solution: The Interplay between State Specific Approaches and a TD-DFT Description. *J. Chem. Theory Comput.* **2015**, *11*, 5782–5790.
- (26) Zinna, F.; Bruhn, T.; Guido, C. A.; Ahrens, J.; Bröring, M.; Di Bari, L.; Pescitelli, G. Circularly Polarized Luminescence from Axially Chiral BODIPY DYEmers: An Experimental and Computational Study. *Chem. - Eur. J.* **2016**, *22*, 16089–16098.
- (27) Sun, H.; Autschbach, J. Electronic Energy Gaps for π -Conjugated Oligomers and Polymers Calculated with Density Functional Theory. *J. Chem. Theory Comput.* **2014**, *11*, 1035–1047.
- (28) Sun, H.; Hu, Z.; Zhong, C.; Chen, X.; Sun, Z.; Brédas, J.-L. Impact of Dielectric Constant on the Singlet–Triplet Gap in Thermally Activated Delayed Fluorescence Materials. *J. Phys. Chem. Lett.* **2017**, *8*, 2393–2398.
- (29) Moral, M.; Muccioli, L.; Son, W.-J.; Olivier, Y.; Sancho-García, J.-C. Theoretical Rationalization of the Singlet–Triplet Gap in OLEDs Materials: Impact of Charge-Transfer Character. *J. Chem. Theory Comput.* **2014**, *11*, 168–177.
- (30) List, N. H.; Zalesný, R.; Murugan, N. A.; Kongsted, J.; Bartkowiak, W.; Ågren, H. Relation between Nonlinear Optical Properties of Push–Pull Molecules and Metric of Charge Transfer Excitations. *J. Chem. Theory Comput.* **2015**, *11*, 4182–4188.
- (31) Humeniuk, A.; Mitrić, R. Long-range correction for tight-binding TD-DFT. *J. Chem. Phys.* **2015**, *143*, 134120–1–21.
- (32) Lu, T.; Chen, F. Multiwfn: A Multifunctional Wavefunction Analyzer. *J. Comput. Chem.* **2012**, *33*, 580–592.
- (33) Le Bahers, T.; Brémond, E.; Ciofini, I.; Adamo, C. The Nature of Vertical Excited States of Dyes Containing Metals for DSSC Applications: Insights from TD-DFT and Density Based Indexes. *Phys. Chem. Chem. Phys.* **2014**, *16*, 14435–14444.
- (34) García, G.; Adamo, C.; Ciofini, I. Evaluating Push–Pull Dye Efficiency Using TD-DFT and Charge Transfer Indices. *Phys. Chem. Chem. Phys.* **2013**, *15*, 20210–20219.
- (35) Ciofini, I.; Le Bahers, T.; Adamo, C.; Odobel, F.; Jacquemin, D. Through-Space Charge Transfer in Rod-like Molecules: Lessons from Theory. *J. Phys. Chem. C* **2012**, *116*, 11946–11955.
- (36) Labat, F.; Le Bahers, T.; Ciofini, I.; Adamo, C. First-Principles Modeling of Dye-Sensitized Solar Cells: Challenges and Perspectives. *Acc. Chem. Res.* **2012**, *45*, 1268–1277.

- (37) Chibani, S.; Le Guennic, B.; Charaf-Eddin, A.; Laurent, A. D.; Jacquemin, D. Revisiting the Optical Signatures of BODIPY with Ab Initio Tools. *Chem. Sci.* **2013**, *4*, 1950–1963.
- (38) Wilbraham, L.; Savarese, M.; Rega, N.; Adamo, C.; Ciofini, I. Describing Excited State Intramolecular Proton Transfer (ESIPT) in Dual Emissive Systems: A Density Functional Theory Based Analysis. *J. Phys. Chem. B* **2014**, *119*, 2459–2466.
- (39) Savarese, M.; Raucci, U.; Adamo, C.; Netti, P.; Ciofini, I.; Rega, N. Non-Radiative Decay Paths in Rhodamines: New Theoretical Insights. *Phys. Chem. Chem. Phys.* **2014**, *16*, 20681–20688.
- (40) Duan, Y.-A.; Geng, Y.; Li, H.-B.; Jin, J.-L.; Wu, Y.; Su, Z.-M. Theoretical Characterization and Design of Small Molecule Donor Material Containing Naphthodithiophene Central Unit for Efficient Organic Solar Cells. *J. Comput. Chem.* **2013**, *34*, 1611–1619.
- (41) Yang, J.; Wang, X.; Yim, W.-L.; Wang, Q. Computational Study on the Intramolecular Charge Separation of D-A- π -A Organic Sensitizers with Different Linker Groups. *J. Phys. Chem. C* **2015**, *119*, 26355–26361.
- (42) Raucci, U.; Savarese, M.; Adamo, C.; Ciofini, I.; Rega, N. Intrinsic and Dynamical Reaction Pathways of an Excited State Proton Transfer. *J. Phys. Chem. B* **2015**, *119*, 2650–2657.
- (43) Savarese, M.; Raucci, U.; Netti, P. A.; Adamo, C.; Rega, N.; Ciofini, I. A Qualitative Model to Identify Non-Radiative Decay Channels: The Spiropyran as Case Study. *Theor. Chem. Acc.* **2016**, *135*, 1–7.
- (44) Frisch, M. J.; Trucks, G. W.; Schlegel, H. B.; Scuseria, G. E.; Robb, M. A.; Cheeseman, J. R.; Scalmani, G.; Barone, V.; Petersson, G. A.; Nakatsuji, H.; et al. *Gaussian 16*, revision A.03; Gaussian, Inc., Wallingford, CT, 2016.
- (45) Jacquemin, D.; Duchemin, I.; Blase, X. 0–0 Energies Using Hybrid Schemes: Benchmarks of TD-DFT, CIS(D), ADC(2), CC2, and BSE/GW Formalisms for 80 Real-Life Compounds. *J. Chem. Theory Comput.* **2015**, *11*, 5340–5359.
- (46) Zhao, Y.; Truhlar, D. G. The M06 Suite of Density Functionals for Main Group Thermochemistry, Thermochemical Kinetics, Non-covalent Interactions, Excited States, and Transition Elements: Two New Functionals and Systematic Testing of Four M06-Class Functionals and 12 Other Function. *Theor. Chem. Acc.* **2008**, *120*, 215–241.
- (47) Perdew, J. P.; Burke, K.; Ernzerhof, M. Generalized Gradient Approximation Made Simple. *Phys. Rev. Lett.* **1997**, *78*, 1396.
- (48) Adamo, C.; Barone, V. Toward Reliable Density Functional Methods without Adjustable Parameters: The PBE0 Model. *J. Chem. Phys.* **1999**, *110*, 6158–6170.
- (49) Chai, J.-D.; Head-Gordon, M. Long-Range Corrected Hybrid Density Functionals with Damped Atom-Atom Dispersion Corrections. *Phys. Chem. Chem. Phys.* **2008**, *10*, 6615–6620.
- (50) Jacquemin, D.; Brémond, E.; Planchat, A.; Ciofini, I.; Adamo, C. TD-DFT Vibronic Couplings in Anthraquinones: From Basis Set and Functional Benchmarks to Applications for Industrial Dyes. *J. Chem. Theory Comput.* **2011**, *7*, 1882–1892.
- (51) Ciofini, I.; Adamo, C. Accurate Evaluation of Valence and Low-Lying Rydberg States with Standard Time-Dependent Density Functional Theory. *J. Phys. Chem. A* **2007**, *111* (25), 5549–5556.
- (52) Martin, R. L. Natural Transition Orbitals. *J. Chem. Phys.* **2003**, *118*, 4775.
- (53) Frisch, M. J.; Trucks, G. W.; Schlegel, H. B.; Scuseria, G. E.; Robb, M. A.; Cheeseman, J. R.; Scalmani, G.; Barone, V.; Mennucci, B.; Petersson, G. A.; et al. *Gaussian 09*, revision A.02; Gaussian, Inc., Wallingford, CT, 2009.
- (54) Le Bahers, T.; Adamo, C.; Ciofini, I. DctViaCube, 2011. www.quanthic.fr.
- (55) Ehara, M.; Fukuda, R.; Adamo, C.; Ciofini, I. Chemically Intuitive Indices for Charge-Transfer Excitation Based on SAC-CI and TD-DFT Calculations. *J. Comput. Chem.* **2013**, *34*, 2498–2501.
- (56) Tognetti, V.; Joubert, L. On the Influence of Density Functional Approximations on Some Local Bader's Atoms-in-Molecules Properties. *J. Phys. Chem. A* **2011**, *115*, 5505–5515.
- (57) Ronca, E.; Angeli, C.; Belpassi, L.; De Angelis, F.; Tarantelli, F.; Pastore, M. Density Relaxation in Time-Dependent Density Functional Theory: Combining Relaxed Density Natural Orbitals and Multireference Perturbation Theories for an Improved Description of Excited States. *J. Chem. Theory Comput.* **2014**, *10*, 4014–4024.
- (58) Pastore, M.; Assfeld, X.; Mosconi, E.; Monari, A.; Etienne, T. Unveiling the Nature of Post-Linear Response Z-Vector Method for Time-Dependent Density Functional Theory. *J. Chem. Phys.* **2017**, *147*, 024108.